Optimization and Engineering (2026) 27:503–530
https://doi.org/10.1007/s11081-025-10016-x

RESEARCH ARTICLE

Robust energy system design via semi-infinite programming

Moritz Wedemeyer[1,2] · Eike Cramer[3] · Alexander Mitsos[1,3,4] · Manuel Dahmen[1]

Received: 22 November 2024 / Revised: 22 May 2025 / Accepted: 13 July 2025 /
Published online: 22 August 2025

Abstract

Time-series information needs to be incorporated into energy system optimization to account for the uncertainty of renewable energy sources. Typically, time-series aggregation methods are used to reduce historical data to a few representative scenarios but they may neglect extreme scenarios, which disproportionally drive the costs in energy system design. We propose the robust energy system design (RESD) approach based on semi-infinite programming and use an adaptive discretization-based algorithm to identify worst-case scenarios during optimization. The RESD approach can guarantee robust designs for problems with nonconvex operational behavior, which current methods cannot achieve. The RESD approach is demonstrated by designing an energy supply system for the island of La Palma. To improve computational performance, principal component analysis is used to reduce the dimensionality of the uncertainty space. The robustness and costs of the approximated problem with significantly reduced dimensionality approximate the full-dimensional solution closely. Even with strong dimensionality reduction, the RESD approach is computationally intense and thus limited to small problems.

Keywords Semi-infinite programming · Robust optimization · Energy system design · Variable renewable energy sources

Abbreviations

BLLP	bi-level linear program
ESIP	existence-constrained semi-infinite program
EGSIP	existence-constrained generalized semi-infinite program

✉ Manuel Dahmen
m.dahmen@fz-juelich.de

[1] Forschungszentrum Jülich GmbH, Institute of Climate and Energy Systems, Energy Systems Engineering (ICE-1), Jülich 52425, Germany

[2] RWTH Aachen University, Aachen 52062, Germany

[3] RWTH Aachen University, Process Systems Engineering (AVT.SVT), Aachen 52074, Germany

[4] JARA-ENERGY, Jülich 52425, Germany

GSIP	generalized semi-infinite program
MILP	mixed-integer linear program
MW	megawatt
NLP	nonlinear program
RESD	robust energy system design
PC	principal component
PCA	principal component analysis
PV	photo voltaic
SIP	semi-infinite program
TAC	total annualized cost
VRES	variable renewable energy sources

Greek Symbols

λ	Lagrange multiplier for equality constraints
μ	Lagrange multiplier for inequality constraints
ϕ	auxiliary variable

Latin Symbols

b	binary variable for on/off decision
e	energy supply gap
e_{epi}	auxiliary variable for energy supply gap
g	inequality constraint
$\mathbf{g}$	vector of inequality constraints
h	equality constraint
$\mathbf{h}$	vector of equality constraints
$\mathcal{L}$	Lagrangian function
n	number
$\mathcal{S}$	set of representative scenarios
$\mathcal{T}$	set of time steps
$\mathbf{w}$	vector of variables for single-level NLP
$\mathcal{W}$	feasible set of variables for single-level NLP
x	design variable
$\mathbf{x}$	vector of design variables
$\mathcal{X}$	feasible set of design variables
y	uncertain variable
$\mathbf{y}$	vector of uncertain variables
$\tilde{\mathbf{y}}$	vector of dependent uncertain variables
$\bar{\mathbf{y}}$	vector of independent uncertain variables
$\mathcal{Y}$	feasible set of uncertain variables
z	operational variable
$\mathbf{z}$	vector of operational variables
$\mathcal{Z}$	feasible set of operational variables

Subscripts

d	data points
e	energy supply gap
en	energy system

eq	equations
i	index
j	index
epi	epigraph reformulation
o	operational costs
p	principal components
ref	reformulation
s	representative scenarios
t	time step
x	design variables
y	uncertain variables
z	operational variables

Nomenclature

Throughout the manuscript, scalar-valued quantities are denoted in regular font, e.g., x, vector-valued quantities are denoted in bold font, e.g., $\mathbf{x}$, and set-valued quantities are denoted in calligraphic font, e.g., $\mathcal{X}$.

1 Introduction

The transformation of energy supply systems from fossil energy sources to variable renewable energy resources (VRES) has increased the volatility of electricity supply and, consequently, demand. This volatility introduced by the stochastic nature of VRES has led to new challenges in the design and operation of energy systems (Gross et al. 2007; Huber et al. 2014; Heptonstall and Gross 2021).

Mathematical optimization is an effective tool to design energy systems that are optimal, e.g., have minimal total annualized cost or global warming impact, and can be leveraged to design energy systems that are robust towards the volatility introduced by VRES (Biegler and Grossmann 2004; Yunt et al. 2008; Lubin et al. 2011; Li and Barton 2015). Optimization has been successfully applied to design energy systems across various scales, from utility systems at the plant scale (Papoulias and Grossmann 1983; Voll et al. 2013; Bahl et al. 2018; Baumgärtner et al. 2019) to energy systems for districts (Bünning et al. 2018; Schütz et al. 2018; Teichgraeber and Brandt 2019) up to power systems on islands (Ma et al. 2014; Gils and Simon 2017; Barone et al. 2021) and on the (inter)-national scale (Kannan and Turton 2013; Siala et al. 2019; Reinert et al. 2020). For a review of modeling tools for renewable energy systems, we refer to Ringkjøb et al. (2018).

Modeling the volatility of VRES leads to uncertainties in the optimization problem parameters. Two popular approaches to account for uncertain parameters are stochastic programming (Dantzig 1955) and robust optimization (Campo and Morari 1987). Stochastic programming requires knowledge of the probability distribution of the uncertain parameters and optimizes the expected value of the objective function. Robust optimization, on the other hand, guarantees the feasibility of an optimal

solution for all parameters within a predefined uncertainty set and does not require the probability distribution. For detailed information on stochastic programming and robust optimization, we refer to Birge and Louveaux (2011) and Ben-Tal et al. (2009), respectively.

To capture the time-varying behavior of VRES, the probability distribution can be approximated discretely by including historical time-series data in the optimization as scenarios in a two-stage stochastic programming (Dantzig 1955) formulation of the design problem (Teichgraeber and Brandt 2022). A sufficiently high temporal resolution is needed to properly account for the time-varying behavior of renewable electricity production (Poncelet et al. 2016; Keles et al. 2017; Ringkjøb et al. 2018). Excessive use of historical data and high temporal resolutions, however, increase the number of constraints and variables of the optimization problem, thus leading to computationally intractable formulations (Pfenninger et al. 2014; Hoffmann et al. 2020). Therefore, tradeoffs between computational tractability and the degree of detail in which the system is modeled are necessary.

Different dimensions of model complexity reduction can be leveraged to facilitate computational tractability. First, model complexity can be reduced by spatial aggregation. A prominent and extreme example is the copper plate assumption, where the spatial distribution is completely ignored, and transmission losses are neglected (Hess et al. 2018). Furthermore, temporal model complexity can be reduced by using only a representative subset of the historical time-series data, e.g., a collection of representative days (Chapaloglou et al. 2022). A popular method to determine representative scenarios is clustering (Kotzur et al. 2018; Teichgraeber and Brandt 2019). However, aggregation methods may neglect extreme scenarios, which may impact the operational feasibility of the optimal system design.

Heuristic methods have been introduced to incorporate extreme scenarios during the design. The heuristics identify and add extreme scenarios to the optimization problem before performing the design optimization. For example, Domínguez-Muñoz et al. (2011) exclude days with peak demands from the aggregation and add these to the scenario data of the problem directly. However, by incorporating individual peak days for the different energy demand forms, e.g., heat, cooling, and electricity, interactions between these demand forms may get lost. Furthermore, when multiple uncertain quantities are considered, e.g., solar electricity production and electricity demand, the worst-case realization might not correspond to scenarios where the quantities are at their extreme values but rather a scenario where the interaction of their values creates the largest supply and demand mismatch.

Furthermore, the worst-case scenario depends on the energy system design; for example, the installed capacities of solar PV and wind turbines in an energy system influence whether scenarios with low wind speeds or low solar irradiance are critical. *A priori* extreme period selection cannot consider this influence of the design on the extreme periods.

To mitigate this problem, extreme periods specific to a given (preliminary) design can be identified by optimizing the system *operation*, i.e., by determining whether the considered design can satisfy energy demands for all historical scenarios. Scenarios in which operations are found to be infeasible are then added as extreme periods to the design problem formulation, and subsequently, another design optimization is

performed. In the context of energy system design, Bahl et al. (2016) introduced such an iterative heuristic in which they repeatedly solve a design problem with approximated operational costs and add virtual time steps for which the operational problem becomes infeasible until eventually a design is obtained that can supply all historical scenarios. The solution approach that Bahl et al. (2016) use to identify worst-case scenarios from a set of finite cardinality is very similar to the algorithm proposed by Blankenship and Falk (1976) to solve semi-infinite programs (SIPs). Teichgraeber et al. (2020) developed this concept further and referred to it as the optimization-based feasibility time-step heuristic. We will refer to this approach as the *feasibility time-step heuristic* for brevity. However, as we will show, considering only the historical data may not be enough to identify robust designs. Specifically, if the operational problem is nonconvex, the identified system design may not be feasible for scenarios that lie "between" historical scenarios, i.e., that constitute convex combinations of historical data.

Addressing the aforementioned challenges, we propose a rigorous and robust energy system design (RESD) approach that identifies worst-case scenarios from a predefined space of possible uncertainty realizations *during* the optimization. The RESD approach bears similarity to the approach for optimal process design under uncertainty by Halemane and Grossmann (1983). We formulate the energy system design problem as a two-stage stochastic program, where we approximate the objective by discretization but treat the constraints continuously by formulating them as semi-infinite constraints (Charnes et al. 1962; Grossmann and Sargent 1978; Hettich and Kortanek 1993; Djelassi et al. 2021). The discretized approximation of the objective is obtained by approximating the operational costs using a small number of representative scenarios that we determine using clustering. To address the neglect of extreme scenarios by clustering, the semi-infinite constraints enforce feasible operation for all scenarios within a predefined uncertainty space and guarantee the robustness of the identified design towards the volatility introduced by the VRES and the energy demand. Semi-infinite programs often arise in robust design problems (Ben-Tal and Nemirovski 2002); for reviews of semi-infinite programming, we refer to Hettich and Kortanek (1993); Rückmann and Reemtsen (1998); Guerra Vázquez et al. (2008); Stein (2012).

The key difference between established methods in energy system design, such as the feasibility time-step heuristic, and the RESD approach is the ability of the latter to consider continuous uncertainty spaces, i.e., allow the sets of possible uncertainty realizations to have infinite cardinality. In contrast, the feasibility time-step heuristic is constrained to finite cardinality sets. The space of uncertainty realizations can be defined arbitrarily; a straightforward example of such a set is a box-constrained set. In the present work, we define the uncertainty space by means of the convex hull around the historical data, i.e., we consider convex combinations of historical data as possible uncertainty realizations.

The optimization problem corresponding to the RESD approach is a three-level hierarchical program that is computationally challenging to solve. If all historical data points are contained within the bounded part of the search space, the optimization problem corresponding to the RESD approach is a restriction of the problem considered in the feasibility time-step heuristic (Bahl et al. 2016; Teichgraeber et al. 2020). A

solution to the restricted problem is robust for more scenarios than the original problem but may have a worse objective function value.

In previous work, we demonstrated that principal component analysis (PCA) is well suited to reduce the dimensionality of energy time-series data (Cramer et al. 2022). To facilitate computational tractability, we use PCA (Pearson 1901) to reduce the dimensionality of the data in the RESD approach. Furthermore, we utilize a lifting approach to improve computational tractability for design problems where the problem of determining the optimal operational strategy is convex. Specifically, we leverage that the lower-level problem is a convex optimization problem to reformulate the problem as a SIP using the approach proposed by Diehl et al. (2013).

The remainder of this work is structured as follows: Section 2 introduces the problem structure associated with the RESD approach and explains how the historical data is incorporated into the optimization problem. In Section 3, we use an illustrative mixed-integer linear problem (MILP) example to demonstrate the shortcomings of the feasibility time-step heuristic in identifying relevant extreme scenarios and demonstrate the robustness of the RESD approach. Furthermore, special cases in which the feasibility time-step heuristic (Bahl et al. 2016; Teichgraeber et al. 2020) yields identical results to the RESD approach are pointed out. Finally, the lifting approach based on Diehl et al. (2013) is introduced to improve computational performance for problems with convex operational behavior. By means of a case study on the La Palma energy system, Section 4 then analyzes the accuracy of the designs obtained by the RESD approach and the influences of the dimensionality reduction and the lifting approach on the computational performance. Finally, Section 5 summarizes our work.

2 Robust energy system design approach

Robust energy system designs are feasible for all considered uncertainty realizations, i.e., they are able to supply the energy demand while satisfying all operational constraints. However, they are not robust with respect to the objective, i.e., they do not give a guaranteed bound on the operational costs. The RESD approach relies on two concepts to identify robust designs that are cost-optimal: (i) the operational costs are estimated using a small number of representative scenarios with associated probabilities of occurrence (Chapaloglou et al. 2022), (ii) an embedded optimization problem ensures the feasibility for all possible uncertainty realizations within a predefined uncertainty set.

$$
\begin{aligned}
\min_{\mathbf{x},\mathbf{z}_s} \quad & \mathit{Investment\ costs}(\mathbf{x}) + \sum_{s\in S} \mathit{Operational\ costs}(\mathbf{z}_s), && \text{(PS)}\\
\text{s.t.} \quad & \mathbf{g}_{en}(\mathbf{x}, \mathbf{y_s}, \mathbf{z}_s) \leq \mathbf{0}\ \forall s \in \mathcal{S} \quad (\mathit{Energy\ system\ model}),\\
& \max_{\mathbf{y}} \min_{\mathbf{z}} \quad \mathit{Energy\ gap}(\mathbf{x}, \mathbf{y}, \mathbf{z}) \leq 0,\\
& \text{s.t.} \quad \mathbf{g}_{en}(\mathbf{x}, \mathbf{y}, \mathbf{z}) \leq \mathbf{0} \quad (\mathit{Energy\ system\ model}),\\
& \qquad \mathbf{g}_{y}(\mathbf{y}) \leq \mathbf{0} \quad (\mathit{Uncertainty\ bounds}),
\end{aligned}
$$

(PS) shows the general structure of the RESD problem. The upper-level problem is the deterministic equivalent of a two-stage stochastic program (Birge and Louveaux 2011) with a discrete approximation of the scenarios by fixed uncertainty realizations $\mathbf{y_s}$ and determines the optimal design decisions $\mathbf{x}$, such as the installed capacities of renewable generators, to achieve a cost-optimal design with respect to the expected value of the operational costs, which is calculated by estimating operational costs with operational decisions $\mathbf{z}_s$. While we assume that the investment costs are not subject to uncertainty, the operational costs depend on future uncertainty realizations, e.g., on the solar irradiance; thus, we estimate their expected value by means of representative scenarios $\mathcal{S}$ (Chapaloglou et al. 2022).

Furthermore, $\mathbf{g}_{en}(\cdot, \cdot, \cdot)$ are the constraints modeling the energy system, which occur both in the upper- and lower-level problem to ensure the feasibility of the operational decisions associated with the representative scenarios and the extreme scenarios.

$$
\begin{aligned}
\max_{\mathbf{y}} \min_{\mathbf{z}} \quad & \mathit{Energy\ gap}(\mathbf{x}, \mathbf{y}, \mathbf{z}) \leq 0, && \text{(MLP)}\\
\text{s.t.} \quad & \mathbf{g}_{en}(\mathbf{x}, \mathbf{y}, \mathbf{z}) \leq \mathbf{0} \quad (\mathit{Energy\ system\ model}),\\
& \mathbf{g}_{y}(\mathbf{y}) \leq \mathbf{0} \quad (\mathit{Uncertainty\ bounds}),
\end{aligned}
$$

To ensure robustness, an embedded optimization problem, which we refer to as the medial-level problem (MLP), guarantees that the energy supply gap is nonpositive for all possible uncertainty realizations $\mathbf{y}$, i.e., the energy supply meets or exceeds the energy demand. This is achieved by identifying the worst-case uncertainty realization for the superordinate design within the predefined uncertainty set defined by $\mathbf{g}_y(\mathbf{y}) \leq \mathbf{0}$. Reaction to the uncertainty realizations, i.e., recourse actions (Birge and Louveaux 2011), is considered through operational decisions $\mathbf{z}$, e.g., battery charge and discharge decisions.

2.1 Processing of historical data

The RESD approach requires representative scenarios for operational cost estimation and uncertainty bounds that delimit the search space for the identification of worst-case uncertainty realizations. We choose to obtain both from historical time-series data.

Figure 1 shows the corresponding data processing step. For each quantity of interest, e.g., solar irradiance, the historical time-series data is split into the desired representative period length, e.g., a representative day.

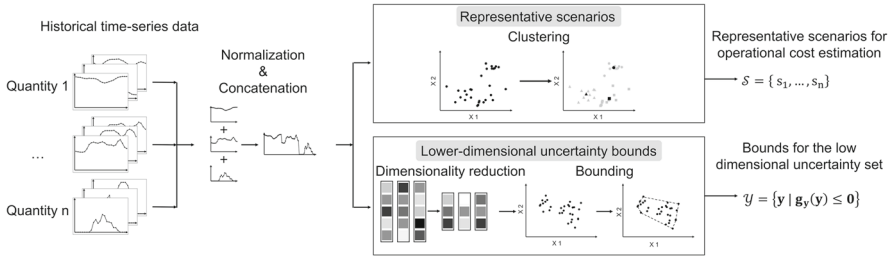

Fig. 1 The processing of historical time-series data to obtain the representative scenarios and uncertainty bounds for the RESD problem: Time-series data with the length of the representative period are collected for different quantities, normalized, and concatenated such that a single vector is obtained for each representative period in the historical data. Representative scenarios are obtained by clustering the concatenated and normalized data according to the framework by Teichgraeber and Brandt (2019). Uncertainty bounds are obtained by first reducing the dimensionality of the historical data and then determining bounds in the lower-dimensional space

First, representative scenarios are chosen according to the framework by Teichgraeber and Brandt (2019), where normalization helps to ensure equal weighting of different quantities during clustering. The normalized time-series data for each attribute, e.g., solar irradiance and electricity demand, are then concatenated, and representative scenarios are selected by clustering. Clustering on the concatenated quantities is necessary to maintain the temporal coherence between different quantities. The choice of the employed normalization technique, clustering method, and parameters is generally problem-specific; we refer to Teichgraeber and Brandt (2019) for guidance.

Second, the bounds for the uncertainty set need to be determined. In previous work, we showed that time-series scenarios for renewable energy sources lie on linear lower-dimensional manifolds (Cramer et al. 2022). Accordingly, we introduce a dimensionality reduction step to facilitate better computational tractability of the RESD problem. The dimensionality reduction shifts the worst-case search to a lower-dimensional latent space, reducing the number of variables in the embedded optimization problem. We choose principal component analysis (PCA) (Pearson 1901) as a linear dimensionality reduction technique. In principle, nonlinear dimensionality reduction methods could be used. However, the corresponding reverse transformation is embedded in the optimization problem. Hence, using a nonlinear reverse transformation gives rise to a nonlinear and, thus, typically much more challenging optimization problem. Depending on the truncation error, the identified extreme scenarios can be more or less extreme in the original space, meaning that the identified designs could be over- or under-conservative.

After reducing the dimensionality of the historical data by a transformation into the principal component space, we need to determine bounds on the lower-dimensional uncertainty realizations. The use of nonlinear bounding techniques would give rise to nonlinear optimization problems. Instead, we choose the convex hull to bound the uncertainty realizations using linear equations. The convex hull can be defined as a convex combination of its vertices or as points that lie inside the combination of half-spaces, i.e., the faces of the convex hull (Avis et al. 1997); we refer to Section

2.2 of the supplementary material for more detailed information. Determining the convex hull has exponential time complexity with respect to the dimensionality of the data (Chazelle 1993), so that for a larger number of principal components the time to compute the convex hull can become a bottleneck, even in comparison to the optimization runtime.

2.2 The RESD approach problem formulation

In the following, constraints are hidden in the sets from which the optimization variables can be chosen for better readability. The (RESD) problem has the following form:

$$\begin{aligned} \min_{\mathbf{x}\in\mathcal{X},\mathbf{z}_s\in\mathcal{Z}_s(\mathbf{x},\mathbf{y_s})} \quad & f(\mathbf{x}) + \sum_{s\in\mathcal{S}} f_o(\mathbf{z}_s), \qquad \text{(RESD)} \\ \text{s.t.} \quad & \max_{\mathbf{y}\in\mathcal{Y}(\mathbf{x})} \min_{\mathbf{z}\in\mathcal{Z}(\mathbf{x},\mathbf{y})} \max_{t\in\mathcal{T}} e_t(\mathbf{x},\mathbf{y},\mathbf{z}) \le 0 \end{aligned}$$

(RESD) is a variant of the problem proposed by Halemane and Grossmann (1983) for optimal process design under uncertainty. It includes a cost function that depends on both design costs $f(\mathbf{x})$ and approximated operational costs $\sum_{s\in\mathcal{S}} f_o(\mathbf{z}_s)$. Furthermore, a constraint enforces feasibility in the worst-case: $\max_{\mathbf{y}\in\mathcal{Y}(\mathbf{x})} \min_{\mathbf{z}\in\mathcal{Z}(\mathbf{x},\mathbf{y})} \max_{t\in\mathcal{T}} e_t(\mathbf{x},\mathbf{y},\mathbf{z}) \le 0$. Here, $\mathbf{x}$ are the design decision variables, e.g., installed PV capacity, and $\mathbf{z}_s$ are the operational decision variables, e.g., battery charging or discharging rates. The subscript s is a scenario index and indicates that $\mathbf{z}_s$ are the operational decisions associated with the respective scenario, while the fixed parameters $\mathbf{y_s}$ are the uncertainty realizations for scenario s.

The robustness of the design is enforced by an embedded optimization problem, which requires that the energy supply gap $e_t(\mathbf{x},\mathbf{y},\mathbf{z})$, i.e., the difference between demand and supply of some energy form, e.g., electricity, has to be nonpositive, i.e., the supply must be equal to or exceed the demand, at all time steps t in the set of considered time steps $\mathcal{T}$. In the case of multiple demands, e.g., electricity and heat ($n = 2$), $e_t(\mathbf{x},\mathbf{y},\mathbf{z})$ will be of the form

$$e_t(\mathbf{x},\mathbf{y},\mathbf{z}) = \max\left(e_{t,1}(\mathbf{x},\mathbf{y},\mathbf{z}),\ldots,e_{t,n}(\mathbf{x},\mathbf{y},\mathbf{z})\right),$$

with n referring to the number of energy forms considered. The inequality constraint requiring the energy supply gap to be nonpositive has to hold for all possible uncertainty realizations $\mathbf{y}$, e.g., capacity factors for PV, while the operational variables $\mathbf{z}$ can be adjusted to help meet the demand.

The set $\mathcal{X} = \{\mathbf{x}\in\mathbb{R}^{n_x} \mid \mathbf{h}_x(\mathbf{x}) = \mathbf{0}, \mathbf{g}_x(\mathbf{x}) \le \mathbf{0}\}$ contains all feasible realizations of the design decisions and the set $\mathcal{Y}(\mathbf{x}) = \{\mathbf{y}\in\mathbb{R}^{n_y} \mid \mathbf{h}_y(\mathbf{x},\mathbf{y}) = \mathbf{0}, \mathbf{g}_y(\mathbf{x},\mathbf{y}) \le \mathbf{0}\}$ describes the feasible set of the uncertainty realizations. Sets $\mathcal{Z}_s(\mathbf{x}) = \{\mathbf{z}_s \in \mathbb{R}^{n_{z_s}} \mid \mathbf{h}_{z_s}(\mathbf{x},\mathbf{y_s},\mathbf{z}_s) = \mathbf{0}, \mathbf{g}_{z_s}(\mathbf{x},\mathbf{y_s},\mathbf{z}_s) \le \mathbf{0}\}$ and $\mathcal{Z}(\mathbf{x},\mathbf{y}) = \{\mathbf{z}\in\mathbb{R}^{n_z} \mid \mathbf{h}_z(\mathbf{x},\mathbf{y},\mathbf{z}) = \mathbf{0}, \mathbf{g}_z(\mathbf{x},\mathbf{y},\mathbf{z}) \le \mathbf{0}\}$ describe feasible operational states and are bounded by equations describing the technical behavior of the system, e.g., equations describing the charging

and discharging capabilities of the battery, which additionally depend on the capacities of the installed components $\mathbf{x}$. The dimensions of the vectors are denoted by n_x, n_{z_s}, n_y, n_z, respectively.

The embedded optimization problem in (RESD) can be replaced by a semi-infinite existence constraint (Djelassi 2020):

$$\max_{\mathbf{y}\in\mathcal{Y}(\mathbf{x})} \min_{\mathbf{z}\in\mathcal{Z}(\mathbf{x},\mathbf{y})} \max_{t\in\mathcal{T}} e_t(\mathbf{x},\mathbf{y},\mathbf{z}) \leq 0 \iff \forall \mathbf{y} \in \mathcal{Y}(\mathbf{x})[\exists\, \mathbf{z} \in \mathcal{Z}(\mathbf{x},\mathbf{y}) : \max_{t\in\mathcal{T}} e_t(\mathbf{x},\mathbf{y},\mathbf{z}) \leq 0]$$

If coupling inequality constraints, i.e., constraints of the form $\mathbf{g}_y(\mathbf{x},\mathbf{y}) \leq \mathbf{0}$ that involve the design decisions $\mathbf{x}$ and the uncertainty realizations $\mathbf{y}$, are present, the resulting problem is an existence-constrained generalized semi-infinite program (EGSIP) which can be solved by solving its existence-constrained semi-infinite program (ESIP) relaxation under some mild assumptions (Mitsos and Tsoukalas 2015).

Note that special care must be taken if coupling equality constraints are present. In the medial-level problem, coupling equality constraints can contain both upper- and medial-level variables: $\mathbf{h}_y(\mathbf{x},\mathbf{y}) = \mathbf{0}$. In the lower-level problem, coupling equality constraints can contain upper- and/or medial-level and lower-level variables: $\mathbf{h}_z(\mathbf{x},\mathbf{y},\mathbf{z}) = \mathbf{0}$. Problems with coupling equality constraints may require specialized algorithms since the convergence of the algorithms employed in this work is no longer guaranteed. However, the coupling equality constraints can be eliminated if they can be rearranged as explicit functions that define some dependent optimization variables as a function of the remaining (independent) variables. For example, consider a medial-level problem with coupling constraints $\mathbf{h}_y(\mathbf{x},\mathbf{y}) = \mathbf{0}$. If the uncertainty realizations $\mathbf{y}$ can be split into a dependent part $\tilde{\mathbf{y}}$ and an independent part $\bar{\mathbf{y}}$ and the coupling equality constraints $\mathbf{h}_y(\mathbf{x},\mathbf{y}) = \mathbf{h}_y(\mathbf{x},\tilde{\mathbf{y}},\bar{\mathbf{y}}) = \mathbf{0}$ can be rearranged into an explicit equation $\tilde{\mathbf{y}} = \tilde{\mathbf{y}}(\mathbf{x},\bar{\mathbf{y}})$, $\tilde{\mathbf{y}}$ can be replaced by $\tilde{\mathbf{y}}(\mathbf{x},\bar{\mathbf{y}})$ everywhere, thus eliminating the dependent variables and removing the coupling equality constraints. Halemane and Grossmann (1983) use this technique to replace the state variables in the operational stage by a function of the design variables, uncertainties, and operational variables. In the case that the coupling constraints cannot be rearranged as an explicit function, methods for solving SIPs containing implicit functions, such as the specialized algorithms proposed by Djelassi et al. (2019) and Stuber and Barton (2015) may be used.

To solve the (RESD) problem, we first reformulate it as an EGSIP and then form the ESIP relaxation, which we solve using the algorithm introduced by Djelassi and Mitsos (2021) and implemented in the libDIPS software package (Zingler et al. 2023). To this end, we transform the embedded optimization problem, i.e., the $\max_{\mathbf{y}\in\mathcal{Y}(\mathbf{x})} \min_{\mathbf{z}\in\mathcal{Z}(\mathbf{x},\mathbf{y})} \max_{t\in\mathcal{T}} e_t(\mathbf{x},\mathbf{y},\mathbf{z})$ problem, into a bi-level problem by introducing an auxiliary variable e_{epi} to the minimization problem, which moves the innermost maximization problem into the constraints of the superordinate minimization problem. Since $\mathcal{T}$ is a finite set, we replace $\max_{t\in\mathcal{T}} e_t(\mathbf{x},\mathbf{y},\mathbf{z}) - e_{epi} \leq 0$ by one equation for each

time step t and obtain the bi-level problem:

$$\begin{aligned} \max_{\mathbf{y}\in\mathcal{Y}(\mathbf{x})\mathbf{z}\in\mathcal{Z}(\mathbf{x},\mathbf{y}),e_{epi}} \quad & e_{epi}, \\ \text{s.t.} \quad & e_t(\mathbf{x},\mathbf{y},\mathbf{z}) - e_{epi} \leq 0 \qquad \forall t \in \mathcal{T} \end{aligned}$$

By including the auxiliary variable e_{epi} and the corresponding constraints in the set of lower-level variables $\mathcal{Z}_{epi}(\mathbf{x},\mathbf{y}) = \{\mathbf{z} \in \mathbb{R}^{n_z}, e_{epi} \in \mathbb{R} | \, \mathbf{h}_z(\mathbf{x},\mathbf{y},\mathbf{z}) = \mathbf{0} \wedge \mathbf{g}_z(\mathbf{x},\mathbf{y},\mathbf{z}) \leq \mathbf{0} \wedge e_t(\mathbf{x},\mathbf{y},\mathbf{z}) - e_{epi} \leq 0 \, \forall t \in \mathcal{T}\}$, we can write the embedded optimization problem as $\max_{\mathbf{y}\in\mathcal{Y}(\mathbf{x})\mathbf{z}\in\mathcal{Z}_{epi}(\mathbf{x},\mathbf{y})} e_{epi}$, and thus obtain for the full design problem:

$$\begin{aligned} \min_{\mathbf{x}\in\mathcal{X},\mathbf{z}_s\in\mathcal{Z}_s(\mathbf{x},\mathbf{y_s})} \quad & f(\mathbf{x}) + \sum_{s\in\mathcal{S}} f_o(\mathbf{z}_s), \\ \text{s.t.} \quad & \max_{\mathbf{y}\in\mathcal{Y}(\mathbf{x})\mathbf{z}\in\mathcal{Z}_{epi}(\mathbf{x},\mathbf{y})} e_{epi} \leq 0 \end{aligned}$$

This problem can now be reformulated as an EGSIP (Djelassi and Mitsos 2021):

$$\begin{aligned} \min_{\mathbf{x}\in\mathcal{X},\mathbf{z}_s\in\mathcal{Z}_s(\mathbf{x},\mathbf{y_s})} \quad & f(\mathbf{x}) + \sum_{s\in\mathcal{S}} f_o(\mathbf{z}_s), \qquad \text{(EGSIP)} \\ \text{s.t.} \quad & \forall \mathbf{y} \in \mathcal{Y}(\mathbf{x})[\exists \, \mathbf{z} \in \mathcal{Z}_{epi}(\mathbf{x},\mathbf{y}) : e_{epi} \leq 0] \end{aligned}$$

Generally, if the lower-level feasible set $\mathcal{Z}(\mathbf{x},\mathbf{y})$ of the (RESD) problem is defined by constraints of the form $\mathbf{g}_z(\mathbf{x},\mathbf{y},\mathbf{z}) \leq \mathbf{0}$, a reformulation of the problem is required to ensure applicability of the ESIP algorithm (Djelassi 2020). This reformulation moves the constraints $\mathbf{g}_z(\mathbf{x},\mathbf{y},\mathbf{z}) \leq \mathbf{0}$ into the objective function, which enables the medial level to identify $\mathbf{y}$ that make the lower-level problem infeasible. However, in problem (EGSIP), the epigraph reformulation constraints $e_t(\mathbf{x},\mathbf{y},\mathbf{z}) - e_{epi} \leq 0 \, \forall t \in \mathcal{T}$ are always feasible if the bounds on e_{epi} are sufficiently large, which we can always guarantee by choosing the bounds appropriately. The guaranteed feasibility of the epigraph constraints allows us to omit the reformulation step for the epigraph reformulation constraints. Similarly, it is not necessary to move constraints of the form $\mathbf{g}_z(\mathbf{x},\mathbf{z}) \leq \mathbf{0}$ into the objective function since $\mathbf{y}$ cannot cause infeasibility of $\mathbf{g}_z(\mathbf{x},\mathbf{z})$. Note that uncertainties typically occurring in energy system design problems are uncertain demand and uncertain generation by renewable energy sources, which enter the problem only in the energy balance, i.e., the objective function of the medial-level problem.

The next step is to form the ESIP relaxation. To this end, we first write problem (EGSIP) equivalently (Djelassi 2020) as

$$\begin{aligned} \min_{\mathbf{x}\in\mathcal{X},\mathbf{z}_s\in\mathcal{Z}_s(\mathbf{x},\mathbf{y_s})} \quad & f(\mathbf{x}) + \sum_{s\in\mathcal{S}} f_o(\mathbf{z}_s), \\ \text{s.t.} \quad & \forall \mathbf{y} \in \mathcal{Y}_{ref}[\exists \, \mathbf{z} \in \mathcal{Z}_{epi}(\mathbf{x},\mathbf{y}) : e_{epi} \leq 0 \vee \mathbf{g}_y(\mathbf{x},\mathbf{y}) > \mathbf{0}], \end{aligned}$$

where $\mathcal{Y}_{ref} = \{\mathbf{y} \in \mathbb{R}^{n_y} | \, \mathbf{h}_y(\mathbf{y}) = \mathbf{0}, \mathbf{g}_y(\mathbf{y}) \leq \mathbf{0}\}$ is the set of possible uncertainty realizations without the inequality constraints that depend on the upper-level variables

$\mathbf{x}$, which instead have been moved into the logical constraint $e_{epi} \leq 0 \vee \mathbf{g}_y(\mathbf{x}, \mathbf{y}) > \mathbf{0}$. This logical constraint describes that either the medial-level problem is feasible and the energy supply gap is nonpositive or the medial-level problem is infeasible, i.e., the set of worst-case uncertainty realizations is empty. In either case, the upper-level problem is feasible. Furthermore, we assume here that the coupling equality constraints $\mathbf{h}_y(\mathbf{x}, \mathbf{y}) = \mathbf{0}$, if they were present, have been removed using the procedure described at the beginning of this Section.

To make the ESIP algorithms available in libDIPS (Zingler et al. 2023) applicable, the strictness of the inequality $-\mathbf{g}_y(\mathbf{x}, \mathbf{y}) < \mathbf{0}$ is relaxed, resulting in an ESIP problem:

$$\begin{aligned} \min_{\mathbf{x}\in\mathcal{X}, \mathbf{z}_s\in\mathcal{Z}_s(\mathbf{x},\mathbf{y_s})} \quad & f(\mathbf{x}) + \sum_{s\in\mathcal{S}} f_o(\mathbf{z}_s), \\ \text{s.t.} \quad & \forall \mathbf{y} \in \mathcal{Y}_{ref}[\exists\, \mathbf{z} \in \mathcal{Z}_{epi}(\mathbf{x}, \mathbf{y}) : e_{epi} \leq 0 \vee -\mathbf{g}_y(\mathbf{x}, \mathbf{y}) \leq \mathbf{0}], \end{aligned}$$

which can also be written as:

$$\begin{aligned} \min_{\mathbf{x}\in\mathcal{X}, \mathbf{z}_s\in\mathcal{Z}_s(\mathbf{x},\mathbf{y_s})} \quad & f(\mathbf{x}) + \sum_{s\in\mathcal{S}} f_o(\mathbf{z}_s), \qquad \text{(ESIP REL)} \\ \text{s.t.} \quad & \forall \mathbf{y} \in \mathcal{Y}_{ref}[\exists\, \mathbf{z} \in \mathcal{Z}_{epi}(\mathbf{x}, \mathbf{y}) : \\ & \min(e_{epi}, -g_{y,j}(\mathbf{x}, \mathbf{y}) \mid j \in \{1, \ldots, n_{g_y}\}) \leq 0] \end{aligned}$$

Note that this relaxation is generally inexact. However, it is established in SIP literature that for all but degenerate cases, the relaxed problem should lead to the same objective value as the original problem Mitsos and Tsoukalas (2015).

For notational convenience, we define $g_e(\mathbf{x}, \mathbf{y}, \mathbf{z}) := \min(e_{epi}, -g_{y,j}(\mathbf{x}, \mathbf{y}) \mid j \in \{1, \ldots, n_{g_y}\})$ and write ESIP REL as:

$$\begin{aligned} \min_{\mathbf{x}\in\mathcal{X}, \mathbf{z}_s\in\mathcal{Z}_s(\mathbf{x},\mathbf{y_s})} \quad & f(\mathbf{x}) + \sum_{s\in\mathcal{S}} f_o(\mathbf{z}_s), \qquad \text{(ESIP)} \\ \text{s.t.} \quad & \forall \mathbf{y} \in \mathcal{Y}_{ref}[\exists\, \mathbf{z} \in \mathcal{Z}_{epi}(\mathbf{x}, \mathbf{y}) : g_e(\mathbf{x}, \mathbf{y}, \mathbf{z}) \leq 0] \end{aligned}$$

The (ESIP) problem determines design decision variables $\mathbf{x}$ and operational decision variables $\mathbf{z}_s$ such that for all feasible uncertainty realizations $\mathbf{y}$ in the set of possible uncertainty realizations $\mathcal{Y}_{ref}$ there exist operational recourse actions $\mathbf{z}$ so that the constraint $g_e(\mathbf{x}, \mathbf{y}, \mathbf{z}) \leq 0$ is satisfied, meaning that either $e_{epi} \leq 0$ is satisfied or one of the EGSIP constraints is violated, i.e., $-g_{y,j}(\mathbf{x}, \mathbf{y}) \leq 0$, and the set of uncertainty realizations of the EGSIP $\mathcal{Y}(\mathbf{x})$ is empty.

3 Limitations of the feasibility time-step heuristic

This section highlights how the feasibility time-step heuristic cannot rigorously provide robust designs for nonconvex problems. Specifically, we showcase in Section 3.1 how the RESD approach can identify a robust design for a nonconvex problem while the feasibility time-step heuristic (Bahl et al. 2016; Teichgraeber et al. 2020) fails.

Section 3.2 shows the cases for which the feasibility time-step heuristic yields robust designs. Finally, in Section 3.3, we present an extension to the RESD approach that improves performance for problems with convex lower-level problem.

3.1 MILP example

Ensuring operability for all historical data may not be enough to obtain a robust design if the operational problem is nonconvex. SIPs with nonconvex lower-level problems are challenging to solve and cannot, in general, be reformulated as finite optimization problems (Djelassi et al. 2021). The reformulation into a tractable finite optimization problem requires the equations and uncertainty set to fulfill special criteria (Bertsimas et al. 2011). MILPs are nonconvex problems and are extensively used in energy system design (Pfenninger et al. 2014). Therefore, we use a small MILP example that mimics an energy system to demonstrate the shortcomings of the feasibility time-step heuristic and solve it using the RESD approach.

The MILP problem reads

$$\begin{aligned} \min_{(x_1,x_2)\in[0,100]^2} \quad & 2x_1 + x_2, && \text{(MILP RESD)} \\ \text{s.t.} \quad & \forall y_1 \in [0, 100][\exists (z_1, z_2, b) \in \mathcal{Z}(x_1, x_2, y_1) : y_1 - z_1 - z_2 \leq 0], \end{aligned}$$

with the feasible set

$$\mathcal{Z}(x_1, x_2, y_1) = \{(z_1, z_2) \in [0, 100]^2, b \in \{0, 1\} \mid z_1 - x_1 \leq 0 \wedge z_2 - bx_2 \leq 0 \wedge 0.2bx_2 - z_2 \leq 0 \wedge y_1 - z_1 - z_2 = 0\}.$$

In (MILP RESD), x_1 and x_2 represent abstract component capacities, y_1 an uncertain demand, and z_1 and z_2 component outputs, while b models on/off decisions for component 2 to account for the minimal part load restriction of that component. Compared with Component 1, Component 2 is half as expensive to install but has a minimum part load, below which the component has to be shut off.

For simplicity, we assume cost and demand data without reference to real-world data. Specifically, Component 1 is assumed to cost 2 units, and Component 2 is assumed to cost 1 unit. Demand is assumed to be in the range between 0 and 100 units and has to be met exactly without curtailment of excess power.

Note that the coupling equality constraint $y_1 - z_1 - z_2 = 0$, which represents the no-curtailment constraint, can be handled by applying the approach described in Section 2.2, i.e., we solve the equality constraint explicitly for z_2 and substitute $z_2 = y_1 - z_1$ to obtain the following problem:

$$\begin{aligned} \min_{(x_1,x_2)\in[0,100]^2} \quad & 2x_1 + x_2, && \text{(MILP FEAS)} \\ \text{s.t.} \quad & \forall y_1 \in [0, 100][\exists (z_1, b) \in \mathcal{Z}_{feas}(x_1, x_2, y_1) : 0 \leq 0], \end{aligned}$$

with the feasible set

$$\mathcal{Z}_{feas}(x_1, x_2, y_1) = \{z_1 \in [0, 100], b \in \{0, 1\} \mid z_1 - x_1 \leq 0 \wedge y_1 - z_1 - bx_2 \leq 0 \wedge 0.2bx_2 - y_1 + z_1 \leq 0\}.$$

When substituting $z_2 = y_1 - z_1$ into the SIP constraint, we obtain the trivial constraint $0 \leq 0$, which is always satisfied if the feasible set $\mathcal{Z}_{feas}(x_1, x_2, y_1)$ is not empty. Hence, (MILP FEAS) ensures that the lower-level feasible set is not empty.

The lower-level feasible set $\mathcal{Z}_{feas}(x_1, x_2, y_1)$ depends on the uncertain variable y_1. As described in Section 2.2, we remove this dependency by moving the constraints into the objective function of the medial- and lower-level problem, i.e.,

$$\begin{aligned} \min_{(x_1,x_2)\in[0,100]^2} \quad & 2x_1 + x_2, && \text{(MILP ESIP REF)} \\ \text{s.t.} \quad & \forall y_1 \in [0, 100][\exists (z_1, b) \in \mathcal{Z}_{ref}(x_1, x_2) : \\ & \max\{y_1 - z_1 - bx_2, 0.2bx_2 - y_1 + z_1\} \leq 0], \end{aligned}$$

with the feasible set

$$\mathcal{Z}_{ref}(x_1) = \{z_1 \in [0, 100], b \in \{0, 1\} \mid z_1 - x_1 \leq 0\}.$$

and solve it using the ESIP algorithm implemented in libDIPS (Zingler et al. 2023). The involved sub-problems and the solver settings can be found in Section 1 and Table 2 of the supplementary material, respectively.

We obtain an optimal system design with $x_1 = 16.60$ and $x_2 = 83.40$, i.e., the capacity of the more expensive Component 1 is roughly 20% of the capacity of Component 2. The fact that the more expensive Component 1 is built allows the system to satisfy the demand below the minimal part load of Component 2.

If only the vertices of the uncertain demand set $\{0, 100\}$ had been considered, the optimal solution would have been $x_1 = 0$ and $x_2 = 100$. However, this solution is not robust to certain possible intermediate demands. For example, the demand $y_1 = 15$ lies below the minimal part load of Component 2, i.e., $0.2 \cdot 100 = 20$. Since Component 1 would have been installed, this demand could not be satisfied.

Note that the nonconvexity introduced by the minimal part load of Component 2 would not lead to infeasibility without the no-curtailment assumption. If curtailment were allowed, Component 2 could be operated at minimal part load for demands smaller than its minimal part load. Consequently, the minimal part load could be neglected in the medial-level problem, effectively removing the nonconvexity. Thus, nonconvexities do not necessarily lead to worst-case scenarios that lie in-between historical scenarios. However, the example highlights that care must be taken when applying the feasibility time-step heuristic (Bahl et al. 2016; Teichgraeber et al. 2020) to nonconvex problems.

3.2 When considering historical data is sufficient

In the previous section, we highlighted how the feasibility time-step heuristic (Bahl et al. 2016; Teichgraeber et al. 2020) may fail for nonconvex problems. However, there are special cases for which the heuristic yields designs that are identical to the ones found by the RESD approach using the convex hull bounding the full dimensional uncertainty space. In these special cases, the objective function $g_e(\mathbf{x}, \mathbf{y}, \mathbf{z})$ and the constraints of the lower-level problem need to be such that worst-case scenarios lie at an extreme point of $\mathcal{Y}_{ref}$. An analogy to this is that the maximum of a convex function lies at an extreme point of its domain. The identified designs are then robust to all uncertainty realizations in the convex hull of the considered historical data.

Worst-case scenarios can then be identified by solving the embedded (MAXMIN) problem, i.e.,

$$\max_{\mathbf{y}\in\mathcal{Y}_{ref}} \min_{\mathbf{z}\in\mathcal{Z}_{epi}(\mathbf{x},\mathbf{y})} g_e(\mathbf{x}, \mathbf{y}, \mathbf{z}), \tag{MAXMIN}$$

using vertex enumeration (Halemane and Grossmann 1983), i.e., the vertices of the feasible set of uncertainty realizations $\mathcal{Y}_{ref}$ are enumerated, and the operational problem is solved for each vertex. It is thus sufficient to examine the historical data that constitute the vertices of the convex hull and unnecessary to consider the entire historical data set, as it is done in the feasibility time-step heuristic.

There are two special cases for which Halemane and Grossmann (1983) and Bialas and Karwan (1982) have proven that the worst-case scenarios lie on the vertices of the feasible set and for which the feasibility time-step heuristic thus leads to robust designs: (i) if the semi-infinite constraint $g_e(\mathbf{x}, \mathbf{y}, \mathbf{z})$ is jointly convex in $\mathbf{y}$ and $\mathbf{z}$ and all other lower-level constraints are convex in $\mathbf{z}$ (Halemane and Grossmann 1983), and (ii) if both the medial-level and the lower-level problem of the (RESD) problem are linear, i.e., the objectives and constraints are linear and consequently the embedded MAXMIN problem is a bilevel linear program (BLLP) (Bialas and Karwan 1982).

3.3 Lifting approach for convex lower-level problems

Finally, we introduce a lifting approach to improve the computational performance of the RESD approach that is applicable if the lower-level problem is convex, i.e., the operational problem is convex. The motivation for this reformulation is that solving (ESIP) using the ESIP algorithm proposed by Djelassi and Mitsos (2021), which is based on the Blankenship and Falk (1976) algorithm, proved to be computationally slow in our preliminary investigations. Specifically, we found that the majority of the CPU time to solve the ESIP was spent on the solution of the embedded optimization problem (MAXMIN), which is equivalent to the semi-infinite existence constraint of (ESIP), i.e., $\forall \mathbf{y} \in \mathcal{Y}_{ref} [\exists\, \mathbf{z} \in \mathcal{Z}_{epi}(\mathbf{x}, \mathbf{y}) : g_e(\mathbf{x}, \mathbf{y}, \mathbf{z}) \leq 0]$.

The lifting approach described in Diehl et al. (2013) allows us to reformulate (MAXMIN) as a single-level nonlinear program (NLP). To this end, we first reformulate (MAXMIN) as a SIP by writing its epigraph reformulation with the auxiliary

variable ϕ (Stein 2003):

$$\begin{aligned} \max_{\mathbf{y}\in\mathcal{Y}_{ref},\phi} \quad & \phi, \\ \text{s.t.} \quad & \phi - g_e(\mathbf{x},\mathbf{y},\mathbf{z}) \leq 0 \; \forall \mathbf{z} \in \mathcal{Z}_{epi}(\mathbf{x},\mathbf{y}) \end{aligned} \tag{ES}$$

We then employ the lifting method (Diehl et al. 2013) to reformulate (ES) into the NLP

$$\begin{aligned} \max_{\mathbf{y}\in\mathcal{Y}_{ref},\mathbf{z}\in\mathcal{Z}_{epi}(\mathbf{x},\mathbf{y}),\phi,\boldsymbol{\lambda},\boldsymbol{\mu}} \quad & \phi, \\ \text{s.t.} \quad & \phi - \mathcal{L}(\mathbf{x},\mathbf{y},\mathbf{z},\boldsymbol{\lambda},\boldsymbol{\mu}) = 0, \\ & \nabla_{\mathbf{z}}\phi - \nabla_{\mathbf{z}}\mathcal{L}(\mathbf{x},\mathbf{y},\mathbf{z},\boldsymbol{\lambda},\boldsymbol{\mu}) = \mathbf{0}, \\ & \boldsymbol{\mu} \geq \mathbf{0}, \\ & \boldsymbol{\mu}^\top \mathbf{g}_z(\mathbf{x},\mathbf{y},\mathbf{z}) = \mathbf{0}, \end{aligned}$$

with Lagrange multipliers $\boldsymbol{\lambda}$ and $\boldsymbol{\mu}$ and

$$\mathcal{L}(\mathbf{x},\mathbf{y},\mathbf{z},\boldsymbol{\lambda},\boldsymbol{\mu}) = g_e(\mathbf{x},\mathbf{y},\mathbf{z}) + \boldsymbol{\lambda}^\top \mathbf{h}_z(\mathbf{z}) + \boldsymbol{\mu}^\top \mathbf{g}_z(\mathbf{x},\mathbf{y},\mathbf{z}).$$

Note that $\nabla_{\mathbf{z}}\phi = 0$ and by substituting ϕ in the objective function using $\phi = \mathcal{L}(\mathbf{x},\mathbf{y},\mathbf{z},\boldsymbol{\lambda},\boldsymbol{\mu})$ we end up with the single-level problem:

$$\begin{aligned} \max_{\mathbf{y}\in\mathcal{Y}_{ref}\mathbf{z}\in\mathcal{Z}_{epi}(\mathbf{x},\mathbf{y}),\boldsymbol{\lambda},\boldsymbol{\mu}} \quad & \mathcal{L}(\mathbf{x},\mathbf{y},\mathbf{z},\boldsymbol{\lambda},\boldsymbol{\mu}), \\ \text{s.t.} \quad & \nabla_{\mathbf{z}}\mathcal{L}(\mathbf{x},\mathbf{y},\mathbf{z},\boldsymbol{\lambda},\boldsymbol{\mu}) = \mathbf{0}, \\ & \boldsymbol{\mu} \geq \mathbf{0}, \\ & \boldsymbol{\mu}^\top \mathbf{g}_z(\mathbf{x},\mathbf{y},\mathbf{z}) = \mathbf{0} \end{aligned} \tag{NLP}$$

The objective is nonlinear because of the multiplication of the Lagrange multipliers $\boldsymbol{\mu}$ and $\boldsymbol{\lambda}$ with the constraints $\mathbf{g}_z(\mathbf{x},\mathbf{y},\mathbf{z})$ and $\mathbf{h}_z(\mathbf{z})$. Note that, contrary to Diehl et al. (2013), we added the nonlinear complementarity constraints $\boldsymbol{\mu}^\top \mathbf{g}_z(\mathbf{x},\mathbf{y},\mathbf{z}) = \mathbf{0}$ since we found this to help convergence in our case study (cf. Section 4). This is an unexpected result since a major motivation of the lifting approach is to avoid the complementarity constraints, which are numerically poorly behaved (Scheel and Scholtes 2000).

Finally, by replacing (MAXMIN) with its single-level reformulation (NLP), we obtain the SIP reformulation of the (RESD), i.e.,

$$\begin{aligned} \min_{\mathbf{x}\in\mathcal{X},\mathbf{z}_s\in\mathcal{Z}_s(\mathbf{x})} \quad & f(\mathbf{x}) + \sum_{s\in\mathcal{S}} f_o(\mathbf{z}_s), \\ \text{s.t.} \quad & \mathcal{L}(\mathbf{x},\mathbf{w}) \leq 0 \; \forall \mathbf{w} \in \mathcal{W}(\mathbf{x}), \end{aligned} \tag{RESD SIP}$$

with

$$\mathcal{W}(\mathbf{x}) = \{\mathbf{y} \in \mathcal{Y}_{ref}, \mathbf{z} \in \mathcal{Z}_{epi}(\mathbf{x}, \mathbf{y}), \boldsymbol{\lambda}, \boldsymbol{\mu} \mid \nabla_{\mathbf{z}} \mathcal{L}(\mathbf{x}, \mathbf{y}, \mathbf{z}, \boldsymbol{\lambda}, \boldsymbol{\mu}) = \mathbf{0},\ \boldsymbol{\mu} \geq \mathbf{0},\ \boldsymbol{\mu}^\top \mathbf{g}_I(\mathbf{x}, \mathbf{y}, \mathbf{z}) = \mathbf{0}\}.$$

(RESD SIP) can be solved using the implementation of the Blankenship & Falk algorithm (Blankenship and Falk 1976) available in libDIPS (Zingler et al. 2023).

4 La Palma energy system

We now analyze how close the lower-dimensional RESD problem approximates the costs of the full-dimensional problem as well as the performance of the RESD approach using the example of determining a robust energy system design for the island of La Palma in the Canary Islands. La Palma is an example of an isolated energy system with significant decarbonization potential. Isolated energy systems are defined by a lack of connection to a superordinate energy grid and, consequently, a necessity for self-sufficiency in electricity production. Due to their maturity and reliability, diesel engines have been the electricity generators of choice for many isolated systems (Kennedy et al. 2017). As of 2021, only 20% of gross electricity production in the whole Canary Islands was supplied by renewable sources, highlighting the presently strong reliance on fossil fuels (Gobierno de Canarias 2023a). Furthermore, the Canary Islands have a high availability of renewable energy resources, especially solar (Meschede et al. 2016), and plans to decarbonize their economy and achieve carbon neutrality by 2040 (Gobierno de Canarias 2023b) have been announced.

We consider the following system components: PV units, wind turbines, diesel generators, and battery systems. We neglect to model the electricity distribution system and the related transmission losses to keep the computational complexity manageable; thus, all system components are directly connected to a single node to supply the island's energy demand.

We use data for wind speed and global irradiance obtained from the Photovoltaic Geographical Information System (PVGIS) by the European Union (European Commission 2022; Huld et al. 2012). Furthermore, electricity demand data was aggregated from the Spanish electricity system operator Red Eléctrica de España (2024). The data covers the timespan from 2013 to 2019 and is separated into single-day periods with an hourly resolution. We use 15 representative scenarios in the approximation of the operational costs, as this number leads to a decent approximation of the load curve (see supplementary materials, Figure 2). Detailed information about the case study, such as the modeling of the individual components, determination of cost parameters, and the overall problem formulation, is provided in Section 2 of the supplementary materials.

The resulting RESD problem has linear medial- and lower-level problems. Hence, the lifting approach (cf. Section 3.3), the vertex enumeration (cf. Section 3.2), and thus also the feasibility time-step heuristic (Bahl et al. 2016; Teichgraeber et al. 2020) are applicable. We utilize the latter as a reference to solve the full-dimensional problem

and compare the solution to those of the RESD approach with different degrees of dimensionality reduction. We do not compare the computational performance of the feasibility time-step heuristic with that of the RESD approach, as the RESD approach is generally applicable, i.e., for nonconvex problems, whereas the feasibility time-step heuristic yields guaranteed robust designs only in the special cases described in Section 3.2.

The full problem formulation and the application of the reformulation steps described in Section 2 to transform the embedded optimization problem into a single-level NLP are provided in the supplementary materials in Sections 2.2 & 2.4. The resulting (ESIP) and (RESD SIP) are solved with the Blankenship & Falk-based ESIP algorithm and the Blankenship & Falk algorithm, respectively, using the implementation in libDIPS (Zingler et al. 2023) and the Gurobi solver version 11.0 (Gurobi Optimization, LLC 2024). We use a desktop computer with a 4-core/4-thread Intel i5-4570 CPU with 3.2GHz/3.6GHz base/turbo frequency and 16GB of RAM running Microsoft Windows 10 Enterprise version 10.0.17763. Optimization settings for libDIPS and Gurobi deviating from the default values are given in Section 3 of the supplementary materials; all 4 cores were allocated to the numerical experiments.

4.1 Optimal robust design

First, we briefly analyze the robust design resulting from the RESD approach and compare it to La Palma's current energy system. Figure 2 shows the mean and the standard deviation of the daily electricity demand. Additionally, the 15 representative scenarios used to approximate the operational costs are shown. The demand varies significantly over the course of a day, with a multiple-hour-long peak in the middle of the day between 08:00 and 12:00 and a sharp peak in the evening around 20:00. The demand data varies between 0.2MW and 44.8MW, with the low value of 0.2MW being associated with a power outage that occurred on December 11th, 2013.

Figure 3 shows the currently installed capacities as well as the capacities of the robust design obtained by the RESD approach using 16 time steps and 9 principal components.

The total annualized costs (TAC) of the RESD design amount to 28.0M€/yr and are comprised of 19.2M€/yr of capital expenses and 8.8M€/yr of operational expenses. The average cost of electricity generation is 105.6€/MWh, compared to the actual average cost of electricity generation in the entire Canary Islands of 161.5€/MWh in 2021 (Gobierno de Canarias 2023a). Note that the current energy system has an overcapacity of conventional diesel generators due to some of the generation capacity being held back as a backup. In the RESD approach, we do not take into account possible component failures.

In the robust design, the majority of electricity is produced by wind turbines with 50.8%, followed by solar with 41.2%, and diesel with 8.0%. Renewable resources are preferred over diesel since they have lower variable operational costs. The high variable operational costs of diesel engines are primarily driven by the price of fuel and the costs of dispatch emission rights, which are described in Section 2.3 of the supplementary material. Compared to the current design, the RESD design exhibits

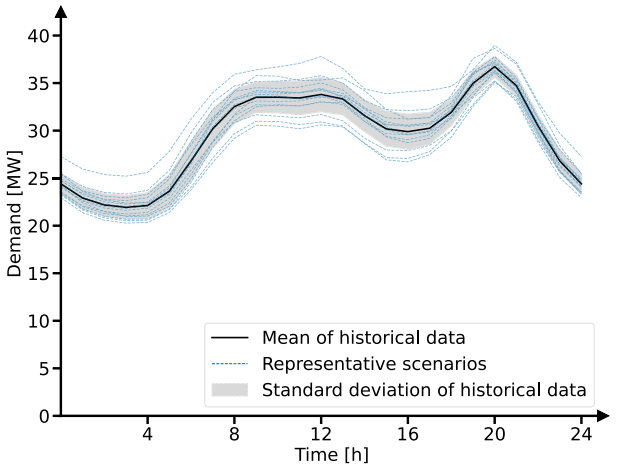

Fig. 2 Mean and standard deviation of the daily historical electricity demand on the island of La Palma in 2013-2019. Demand data were obtained from the Spanish electricity distribution system operator Red Eléctrica de España (2024). Furthermore, the 15 representative scenarios used to compute the operational costs are depicted as dashed lines. There is significant variation in demand over the course of a day, with a wide peak during the morning and a sharp peak in the evening

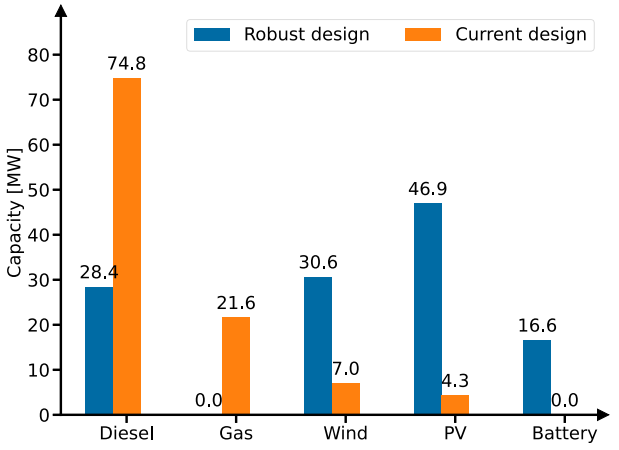

Fig. 3 Installed component capacities for the robust design (blue) identified by the RESD approach using 16 time steps and 9 principal components. For comparison, the currently installed capacities (orange) (Gobierno de Canarias 2023a) are shown. The current design has much higher conventional generation capacity. However, plans to switch to higher renewable electricity generation have already been announced (Gobierno de Canarias 2023b). Note that we did not consider possible component failures in the RESD approach, and hence do not have backup capacities, which are considered in the current design

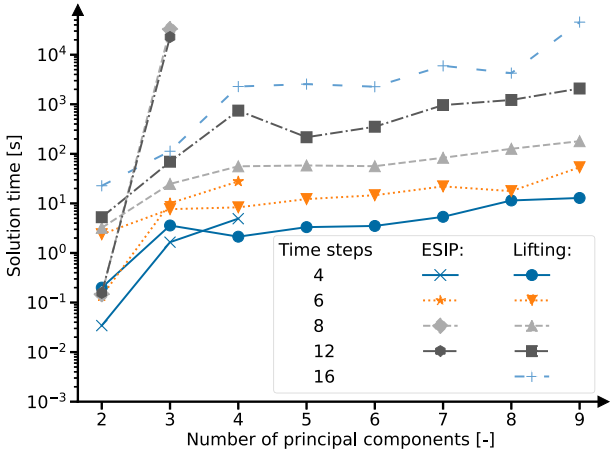

Fig. 4 Average solution times in logarithmic scale for the ESIP and the lifting approach. The average solution time in seconds is plotted against the number of principal components (PCs) for varying numbers of time steps. The solution time increases both with an increasing number of PCs and time steps. The lifting approach scales better with an increasing number of PCs than the ESIP approach

a much higher share of renewable generation, with the renewable energy penetration reaching 92.0%. In comparison, only 10.3% of gross electricity production in La Palma was supplied by renewable sources in 2021 (Gobierno de Canarias 2023a).

4.2 Performance and accuracy

We run the La Palma case study for different numbers of time steps and principal components (PCs). Varying the latter parameter allows us to determine how the dimensionality reduction influences the computational performance and the accuracy of the obtained results. We always use five random seeds for the Gurobi optimizer (Gurobi Optimization, LLC 2024) and average the obtained solution times since solution times can vary strongly with random seeds depending on the nodes explored by the branch and bound algorithm. We measure the solution time by taking the 'CPU time' reported by libDIPS (Zingler et al. 2023), which is the sum of the wall-clock times reported by Gurobi (Gurobi Optimization, LLC 2024) for all sub-problems. Note that we did not account for the time it takes to calculate the convex hull in the performance evaluations. As mentioned in Section 2.1, with larger latent space dimensionality, the time to compute the convex hull can become significant compared to the solution time. Hence, we limited the maximum number of principal components in our numerical experiments to 9.

Figure 4 shows the average solution time for the ESIP and the lifting approach for different numbers of PCs and time steps.

As expected, the solution time increases with an increasing number of time steps and PCs. The ESIP approach shows a very strong increase in the solution time with an increasing number of PCs. In fact, we could not obtain results for four or more components with the ESIP approach since the run times became too long. The lift-

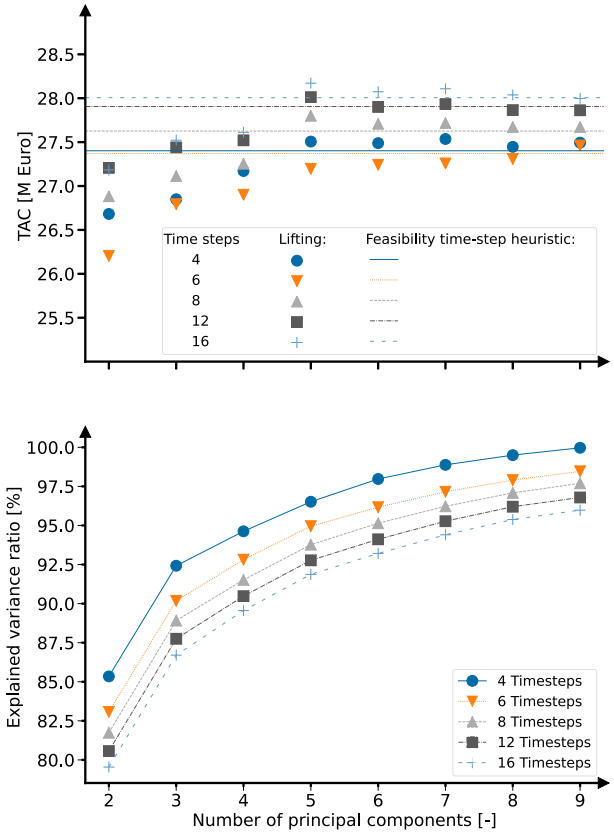

Fig. 5 Optimal total annualized cost (TAC) of energy system designs obtained using the lifting approach against the number of principal components (PCs) for varying number of time steps (top). Dashed lines show results obtained with the feasibility time-step heuristic (Bahl et al. 2016; Teichgraeber et al. 2020) discussed in Section 3.2. For a low number of PCs, a significant approximation error can be seen. If the number of PCs is chosen sufficiently large, i.e., greater than or equal to 5, the TAC of full-dimensional problems is approximated closely by the RESD approach. Explained variance ratio plotted against the number of PCs for a varying number of time steps (bottom). A small number of PCs can explain a majority of the variance in the historical data

ing approach outperforms the ESIP approach if more than two PCs are used. There is a significant increase in solution time between two and three components. Afterward, solution time increases more slowly with an increasing number of components. Furthermore, higher temporal resolutions strongly increase solution times.

The top of Figure 5 shows the optimal TACs of the energy system designs obtained using the lifting approach plotted against the number of PCs for a varying number of time steps. As a reference, the results obtained using the feasibility time-step heuristic (Bahl et al. 2016; Teichgraeber et al. 2020) described in Section 3.2 are shown. The bottom shows the explained variance ratio.

If the number of PCs is small, the RESD designs have lower TACs than the designs resulting from the heuristic. This indicates that, for a small number of PCs, the trunca-

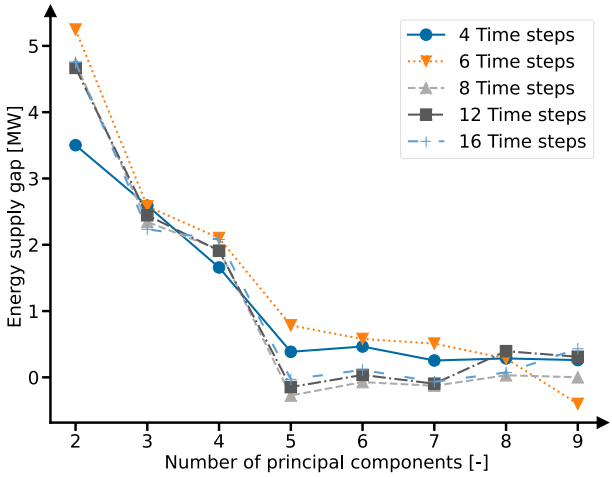

Fig. 6 The maximum energy supply gap for RESD designs with different time resolutions obtained using the lifting approach, calculated by solving the operational problem for all historical data points, is plotted against the number of principal components (PCs). The supply gap is large for a small number of PCs, showing that these designs are not robust. The energy supply gap decreases quickly with an increase in the number of PCs and levels off close to 0MW at 5 PCs, indicating robust designs

tion error from the dimensionality reduction leads to designs that are not robust. With an increasing number of PCs, the TAC of the RESD designs quickly approach those of the designs resulting from the heuristic. In some cases, the TACs of the RESD designs exceed those of the designs obtained by the heuristic, indicating that the truncation error can also lead to overly robust designs. Note that relatively few PCs are needed to account for a majority of the variance in the historical data. With 5 PCs, more than 90% of the variance are explained for all time resolutions. We observe that the TAC of the full-dimensional problem are approximated closely for all time resolutions if the number of PCs is chosen such that the explained variance is above 95%.

Figure 6 shows the energy supply gap over the number of PCs for different time resolutions. The energy supply gap is calculated by solving the operational problem for each historical data point and selecting the maximum constraint violation.

For a small number of PCs, the energy supply gap is large, i.e., in the order of multiple megawatts, showing that these designs are not robust. This finding highlights the tradeoff between a sufficiently accurate approximation of the time-series data and the computational performance. Importantly, the energy supply gap decreases quickly with an increase in the number of PCs and levels off around 5 PCs. In fact, for 48 dimensional data, i.e., 16 time steps and 3 quantities (solar, wind, demand), 6 PCs are sufficient to achieve an appropriate approximation of the full-dimensional problem and hence a robust design. In some cases, the energy supply gap even becomes negative, indicating an overly robust design. This is in accordance with the observation that the TACs for these numbers of PCs are higher than the respective TACs for the designs obtained by the heuristic.

Choosing the right dimensionality of the latent space is difficult in the case of a nonconvex problem. However, we note that the energy supply gap approaches zero for

designs that were obtained with a latent space dimensionality that covers more than 95% of the variance in the historical data. Hence, the explained variance ratio may be used as an indicator to decide on an appropiate dimensionality of the latent space.

5 Conclusion

Uncertainties introduced by VRES should be incorporated into the design of energy systems. Previously *a priori* heuristics, e.g., statistical selection of extreme periods (Domínguez-Muñoz et al. 2011), or optimization-based heuristics, e.g., the feasibility time-step heuristic (Bahl et al. 2016; Teichgraeber et al. 2020), have been proposed. However, *a priori* methods cannot identify extreme periods specific to the energy system because they are agnostic to its design. Moreover, optimization-based heuristics may fail if the design problem exhibits a nonconvex operational problem, e.g., a MILP resulting from the need to model minimal part loads.

We present the robust energy system design (RESD) approach, a rigorous but computationally intense approach to identify extreme scenarios during the design optimization. Specifically, we introduce a semi-infinite existence constraint to the energy system design problem to ensure robustness with respect to uncertainties, resulting in a tri-level optimization problem.

Our RESD approach for the identification of worst-case scenarios during optimization can be seen as a generalization of the finite optimization problem corresponding to the feasibility time-step heuristic (Bahl et al. 2016; Teichgraeber et al. 2020), which determines the constraint violation for all historical scenarios and iteratively adds scenarios with infeasible time steps as extreme scenarios. However, as we have discussed, it is only sufficient to check operability with the historical data, or more specifically, all the scenarios that define the boundary of the convex hull of the historical data, in the case of linear medial- and lower-level problems or jointly convex medial- and lower-level problems. The computational performance of the iterative feasibility time-step heuristic could potentially be improved by using a preprocessing step to identify and discard some or all data points in the interior. In contrast, our RESD approach is dedicated to the more general nonconvex case. The MILP example in Section 3.1 demonstrates how components with minimal part load in combination with a no-curtailment constraint can lead to worst-case scenarios that lie between historical data and not on the vertices of the uncertainty set. Future work should examine to which extent the worst-case scenarios for realistic multi-energy systems, which allow for some curtailment and/or contain storage components, also do not lie on the vertices of the uncertainty set.

Different uncertainty-bounding methods can be used in the RESD approach. In the present contribution, we consider the convex hull of the historical data as the possible uncertainty set, taking advantage of the fact that the describing equations are linear. Still, the computational effort for solving the RESD problem increases quickly with an increasing number of time steps.

Computational tractability can be improved by leveraging dimensionality reduction techniques such as principal component analysis (PCA). While we observe that robust designs can be obtained even in the presence of rather aggressive dimensionality

reduction, the use of PCA inherently introduces an approximation error that can lead to overly or underly robust designs. A suitable dimensionality of the latent space must be found empirically, and in the nonconvex case, a rigorous criterion for validating the robustness of an obtained design is missing. However, the explained variance ratio can be used as an indicator in guiding the selection of an appropriate latent space dimensionality. Specifically, we found designs obtained with a latent space dimensionality covering more than 95% of the variance of the historical data to yield TACs that are close to the TAC of the full-dimensional design.

Although the lifting approach can improve performance if the considered design problem has an embedded convex operational problem, the applicability of the RESD approach is currently limited to small problems due to the involved computational intensity. Furthermore, we found that including the complementarity constraints improves the performance of the lifting approach. This is an unexpected result, and it should be investigated if this holds generally. Wider applicability of our approach could be enabled by faster methods for solving hierarchical programs. For example, the approach by Seidel and Küfer (2022) that improves the rate of convergence of the adaptive discretization approach could reduce the long solution times of the embedded MaxMin problem. Furthermore, the integration of bounding approaches that can handle nonconvexities in the historical data, e.g., holes, as well as the use of nonlinear dimensionality reduction techniques, e.g., autoencoders (Kramer 1991), should be investigated.

Supplementary Information The online version contains supplementary material available at https://doi.org/10.1007/s11081-025-10016-x.

Acknowledgements During the preparation of this work, M.W. used Grammarly to correct grammar and spelling and improve the writing style. After using this tool, all authors reviewed and edited the content as needed and take full responsibility for the content of the publication.

Author Contributions Conceptualization: M.W., E.C., A.M., M.D.; Methodology: M.W.; Software: M.W.; Investigation: M.W.; Visualization: M.W.; Writing - original draft: M.W.; Writing - review & editing: E.C., A.M., M.D.; Supervision: A.M., M.D.; Funding acquisition: A.M., M.D.

Funding Open Access funding enabled and organized by Projekt DEAL. This work was performed as part of the Helmholtz School for Data Science in Life, Earth and Energy (HDS-LEE) and received funding from the Helmholtz Association of German Research Centers.
The authors gratefully acknowledge the financial support of the Kopernikus project SynErgie by the German Federal Ministry of Education and Research (BMBF) and the project supervision by the project management organization Projektträger Jülich (PtJ).

Data Availability The cost parameters for the La Palma case study are collected in Table 1 in the supplementary material, and a detailed description of how they were obtained can be found in Section 2.3 of the supplementary material. The solar irradiance and wind speed data used in the La Palma case study are available at https://re.jrc.ec.europa.eu/pvg_tools/en/. The demand data for La Palma island is available at https://demanda.ree.es/visiona/canarias/la_palma5m/tablas. The wind turbine power curve data for an Enercon E-82 E2 turbine was used. While the data is no longer available on the official manufacturer site, a copy of the data sheet is accessible at https://catalystresearch.wordpress.com/wp-content/uploads/2013/11/enercon_pu_en.pdf.

Declarations

Ethics Approval and Consent to Participate Not applicable.

Consent for Publication Not applicable.

Competing Interests The authors have no relevant financial or non-financial interests to disclose.

References

Avis D, Bremner D, Seidel R (1997) How good are convex hull algorithms? Comput Geom 7(5):265–301

Bahl B, Kümpel A, Lampe M, Bardow A (2016) Time-series aggregation for synthesis of distributed energy supply systems by bounding error in operational expenditure. In: Kravanja Z, Bogataj M (eds) Computer Aided Chemical Engineering, volume 38 of 26 European Symposium on Computer Aided Process Engineering. Elsevier, pp 793–798

Bahl B, Lützow J, Shu D, Hollermann DE, Lampe M, Hennen M, Bardow A (2018) Rigorous synthesis of energy systems by decomposition via time-series aggregation. Computers & Chemical Engineering 112:70–81

Barone G, Buonomano A, Forzano C, Giuzio GF, Palombo A (2021) Supporting the Sustainable Energy Transition in the Canary Islands: Simulation and Optimization of Multiple Energy System Layouts and Economic Scenarios. Frontiers in Sustainable Cities 3:685525

Baumgärtner NJ, Temme F, Bahl B, Hennen MR, Hollermann DE, Bardow A (2019) RiSES4 : Rigorous Synthesis of Energy Supply Systems with Seasonal Storage by relaxation and time-series aggregation to typical periods. In Proceedings of the International Conference on Efficiency, Cost, Optimization, Simulation and Environmental Impact of Energy Systems (ECOS 2019), pages 263–274, Gliwice. Institute of Thermal Technology

Ben-Tal A, El Ghaoui L, Nemirovski AS (2009) Robust Optimization. Princeton Series in Applied Mathematics. Princeton University Press, Princeton

Ben-Tal A, Nemirovski A (2002) Robust optimization - methodology and applications. Math Program 92(3):453–480

Bertsimas D, Brown DB, Caramanis C (2011) Theory and Applications of Robust Optimization. SIAM Rev 53(3):464–501

Bialas W, Karwan M (1982) On two-level optimization. IEEE Trans Autom Control 27(1):211–214

Biegler L, Grossmann I (2004) Retrospective on optimization. Comput Chem Eng 28(8):1169–1192

Birge JR, Louveaux F (2011) Introduction to Stochastic Programming. SpringerLink Bücher, Springer, New York, New York, NY

Blankenship JW, Falk JE (1976) Infinitely constrained optimization problems. J Optim Theory Appl 19(2):261–281

Bünning F, Wetter M, Fuchs M, Müller D (2018) Bidirectional low temperature district energy systems with agent-based control: Performance comparison and operation optimization. Appl Energy 209:502–515

Campo PJ, Morari M (1987) Robust Model Predictive Control. In 1987 American Control Conference, pages 1021–1026

Chapaloglou S, Varagnolo D, Marra F, Tedeschi E (2022) Data-informed scenario generation for statistically stable energy storage sizing in isolated power systems. Journal of Energy Storage 51:104311

Charnes A, Cooper WW, Kortanek K (1962) Duality, haar programs, and finite sequence spaces. Proc Natl Acad Sci 48(5):783–786

Chazelle B (1993) An optimal convex hull algorithm in any fixed dimension. Discrete & Computational Geometry 10(4):377–409
Cramer E, Mitsos A, Tempone R, Dahmen M (2022) Principal component density estimation for scenario generation using normalizing flows. Data-Centric Engineering 3:e7
Dantzig GB (1955) Linear Programming under Uncertainty. Manage Sci 1(3/4):197–206
Diehl M, Houska B, Stein O, Steuermann P (2013) A lifting method for generalized semi-infinite programs based on lower level Wolfe duality. Comput Optim Appl 54(1):189–210
Djelassi H (2020) Diskretisierungsbasierte Algorithmen für die globale Lösung hierarchischer Optimierungsprobleme. Dissertation, RWTH Aachen University
Djelassi H, Glass M, Mitsos A (2019) Discretization-based algorithms for generalized semi-infinite and bilevel programs with coupling equality constraints. J Global Optim 75(2):341–392
Djelassi H, Mitsos A (2021) Global Solution of Semi-infinite Programs with Existence Constraints. J Optim Theory Appl 188(3):863–881
Djelassi H, Mitsos A, Stein O (2021) Recent advances in nonconvex semi-infinite programming: Applications and algorithms. EURO Journal on Computational Optimization 9:100006
Domínguez-Muñoz F, Cejudo-López JM, Carrillo-Andrés A, Gallardo-Salazar M (2011) Selection of typical demand days for CHP optimization. Energy and Buildings 43(11):3036–3043
European Commission (2022) JRC Photovoltaic Geographical Information System (PVGIS). https://re.jrc.ec.europa.eu/pvg_tools/en/. Accessed: 2024-11-12
Gils HC, Simon S (2017) Carbon neutral archipelago - 100% renewable energy supply for the Canary Islands. Appl Energy 188:342–355
Gobierno de Canarias (2023) Anuario Energetico De Canarias 2021. https://www.gobiernodecanarias.org/energia/descargas/SDE/Portal/Publicaciones/AnuarioEnergeticodeCanarias_2021_v2.pdf, Accessed: 2024-11-20
Gobierno de Canarias (2023) Consejería de Transición Ecológica, Lucha contra el Cambio Climático y Planificación Territorial. https://www.gobiernodecanarias.org/boc/2023/104/009.html, Accessed: 2024-11-12
Gross R, Heptonstall P, Leach M, Anderson D, Green T, Skea J (2007) Renewables and the grid: Understanding intermittency. Proceedings of the Institution of Civil Engineers - Energy 160(1):31–41
Grossmann IE, Sargent RWH (1978) Optimum design of chemical plants with uncertain parameters. AIChE J 24(6):1021–1028
Guerra Vázquez F, Rückmann J-J, Stein O, Still G (2008) Generalized semi-infinite programming: A tutorial. J Comput Appl Math 217(2):394–419
Gurobi Optimization, LLC (2024) Gurobi optimizer reference manual. https://www.gurobi.com
Halemane KP, Grossmann IE (1983) Optimal process design under uncertainty. AIChE J 29(3):425–433
Heptonstall PJ, Gross RJK (2021) A systematic review of the costs and impacts of integrating variable renewables into power grids. Nat Energy 6(1):72–83
Hess D, Wetzel M, Cao K-K (2018) Representing node-internal transmission and distribution grids in energy system models. Renewable Energy 119:874–890
Hettich R, Kortanek KO (1993) Semi-Infinite Programming: Theory, Methods, and Applications. SIAM Rev 35(3):380–429
Hoffmann M, Kotzur L, Stolten D, Robinius M (2020) A Review on Time Series Aggregation Methods for Energy System Models. Energies 13(3):641
Huber M, Dimkova D, Hamacher T (2014) Integration of wind and solar power in Europe: Assessment of flexibility requirements. Energy 69:236–246
Huld T, Müller R, Gambardella A (2012) A new solar radiation database for estimating PV performance in Europe and Africa. Sol Energy 86(6):1803–1815
Kannan R, Turton H (2013) A Long-Term Electricity Dispatch Model with the TIMES Framework. Environmental Modeling & Assessment 18(3):325–343
Keles D, Jochem P, McKenna R, Ruppert M, Fichtner W (2017) Meeting the Modeling Needs of Future Energy Systems. Energ Technol 5(7):1007–1025
Kennedy N, Miao C, Wu Q, Wang Y, Ji J, Roskilly T (2017) Optimal Hybrid Power System Using Renewables and Hydrogen for an Isolated Island in the UK. Energy Procedia 105:1388–1393
Kotzur L, Markewitz P, Robinius M, Stolten D (2018) Impact of different time series aggregation methods on optimal energy system design. Renewable Energy 117:474–487
Kramer MA (1991) Nonlinear principal component analysis using autoassociative neural networks. AIChE J 37(2):233–243

Li X, Barton PI (2015) Optimal design and operation of energy systems under uncertainty. J Process Control 30:1–9
Lubin M, Petra CG, Anitescu M, Zavala V (2011) Scalable stochastic optimization of complex energy systems. In Proceedings of 2011 International Conference for High Performance Computing, Networking, Storage and Analysis, SC '11, New York, NY, USA. Association for Computing Machinery
Ma T, Yang H, Lu L (2014) A feasibility study of a stand-alone hybrid solar-wind-battery system for a remote island. Appl Energy 121:149–158
Meschede H, Holzapfel P, Kadelbach F, Hesselbach J (2016) Classification of global island regarding the opportunity of using RES. Appl Energy 175:251–258
Mitsos A, Tsoukalas A (2015) Global optimization of generalized semi-infinite programs via restriction of the right hand side. J Global Optim 61(1):1–17
Papoulias SA, Grossmann IE (1983) A structural optimization approach in process synthesis–I: Utility systems. Computers & Chemical Engineering 7(6):695–706
Pearson K (1901) On lines and planes of closest fit to systems of points in space. The London Edinburgh and Dublin Philosophical Magazine and Journal of Science 2(11):559–572
Pfenninger S, Hawkes A, Keirstead J (2014) Energy systems modeling for twenty-first century energy challenges. Renew Sustain Energy Rev 33:74–86
Poncelet K, Delarue E, Six D, Duerinck J, D'haeseleer W (2016) Impact of the level of temporal and operational detail in energy-system planning models. Appl Energy 162:631–643
Red Eléctrica de España (2024) La Palma - Electricity demand tracking in real time. https://demanda.ree.es/visiona/canarias/la_palma5m/tablas. Accessed: 2024-11-12
Reinert C, Deutz S, Minten H, Dörpinghaus L, von Pfingsten S, Baumgärtner N, Bardow A (2020) Environmental Impacts of the Future German Energy System from Integrated Energy Systems Optimization and Life Cycle Assessment. In: Pierucci S, Manenti F, Bozzano GL, Manca D (eds) Computer Aided Chemical Engineering, volume 48 of 30 European Symposium on Computer Aided Process Engineering. Elsevier, pp 241–246
Ringkjøb H-K, Haugan PM, Solbrekke IM (2018) A review of modelling tools for energy and electricity systems with large shares of variable renewables. Renew Sustain Energy Rev 96:440–459
Rückmann J-J, Reemtsen R, editors (1998) Semi-Infinite Programming, volume 25 of Springer eBook Collection Mathematics and Statistics. Springer, Boston, MA
Scheel H, Scholtes S (2000) Mathematical Programs with Complementarity Constraints: Stationarity, Optimality, and Sensitivity. Math Oper Res 25(1):1–22
Schütz T, Hu X, Fuchs M, Müller D (2018) Optimal design of decentralized energy conversion systems for smart microgrids using decomposition methods. Energy 156:250–263
Seidel T, Küfer K-H (2022) An adaptive discretization method solving semi-infinite optimization problems with quadratic rate of convergence. Optimization 71(8):2211–2239
Siala K, de la Rúa C, Lechón Y, Hamacher T (2019) Towards a sustainable European energy system: Linking optimization models with multi-regional input-output analysis. Energ Strat Rev 26:100391
Stein O (2003) Bi-Level Strategies in Semi-infinite Programming, volume 71 of Nonconvex Optimization and Its Applications. Springer Science+Business Media, New York, NY, softcover repr. of the hardcover 1. ed. edition
Stein O (2012) How to solve a semi-infinite optimization problem. Eur J Oper Res 223(2):312–320
Stuber MD, Barton PI (2015) Semi-Infinite Optimization with Implicit Functions. Industrial & Engineering Chemistry Research 54(1):307–317
Teichgraeber H, Brandt AR (2019) Clustering methods to find representative periods for the optimization of energy systems: An initial framework and comparison. Appl Energy 239:1283–1293
Teichgraeber H, Brandt AR (2022) Time-series aggregation for the optimization of energy systems: Goals, challenges, approaches, and opportunities. Renew Sustain Energy Rev 157:111984
Teichgraeber H, Lindenmeyer CP, Baumgärtner N, Kotzur L, Stolten D, Robinius M, Bardow A, Brandt AR (2020) Extreme events in time series aggregation: A case study for optimal residential energy supply systems. Appl Energy 275:115223
Voll P, Klaffke C, Hennen M, Bardow A (2013) Automated superstructure-based synthesis and optimization of distributed energy supply systems. Energy 50:374–388
Yunt M, Chachuat B, Mitsos A, Barton PI (2008) Designing man-portable power generation systems for varying power demand. AIChE J 54(5):1254–1269
Zingler A, Mitsos A, Jungen D, Djelassi H (2023) libDIPS — Discretization-Based Semi-Infinite and Bilevel Programming Solvers. Optimization Online, 24914